Radiation transfer, Level and Free-electron kinetics in Non-equilibrium Atomic Hydrogen Plasma

Gianpiero Colonna*, Giuliano D'Ammando†, Lucia Daniela Pietanza** and Mario Capitelli‡

*CNR-IMIP, sede di Bari, Via Amendola 122/D, 70126, Bari, Italy, e-mail: gianpiero.colonna@ba.imip.cnr.it
†Dipartimento di Chimica, Universitá di Bari, Via Orabona, 4, 70126, Bari, Italy, e-mail: g.dammando@chimica.uniba.it
**CNR-IMIP, sede di Bari, Via Amendola 122/D, 70126, Bari, Italy, e-mail: daniela.pietanza@ba.imip.cnr.it
‡Dipartimento di Chimica, Universitá di Bari, Via Orabona, 4, 70126, Bari, Italy, e-mail: mario.capitelli@ba.imip.cnr.it

Abstract. In this paper, the absorption coefficient and emissivity of non-equilibrium atomic hydrogen plasma have been calculated in the case of a steady state shock wave. For this purpose, the atomic level population profiles along the shock wave have been calculated using a collisional-radiative model coupled with the electron Boltzmann equation. The spectral coefficients are in turn the input for solving a one-dimensional radiative transfer equation, which allows to calculate the radiation intensity and radiative flux in the plasma slab.

Keywords: state-to-state kinetics

INTRODUCTION

To describe the spectra emitted by a plasma in shock wave conditions, thermo-chemical non-equilibrium should be taken into account. Usually, the absorption coefficient and emissivity are calculated assuming the level population densities to be described by a Boltzmann distribution at the temperature associated to the particular degree of freedom (multi-temperature plasma). However, accurate investigation based on state-to-state kinetics [1] shows that internal level populations are strongly affected by ionization resulting in the depletion of higher excited levels respect to Boltzmann. The underpopulation of these levels lowers the plasma emissivity [2]. These aspects have been already investigated using a zero-dimensional time dependent collisional-radiative model where shock wave conditions were approximated by imposing an abrupt increase of the gas temperature [2]. In this paper, we have improved the model by coupling the solution of the one dimensional steady-state continuity equations with the collisional-radiative model. In this way, spatial profiles for plasma composition and level densities can be calculated and used as input data for the one-dimensional radiative transfer equation to determine the radiation energy and fluxes.

MODEL DESCRIPTION

The hydrodynamic description of the shock wave is studied using the steady state continuity equations [3, 4, 5], while plasma composition, H level and electron kinetics are described with a collisional-radiative model and the electron Boltzmann equation. Finally the radiative field is determined using the radiative transfer equation. In this section we briefly describe each of these methods.

Steady-state shock wave continuity equation

A shock waves is characterized by a rapid rise in pressure, temperature and density of the flow. In experimental studies of nozzle flow, steady state conditions are achieved and the following conservation laws for mass density, momentum and energy fluxes can be applied:

$$\rho_1 u_1 = \rho_2 u_2 = c_1 \tag{1}$$

$$\rho_1 u_1^2 + P_1 = \rho_2 u_2^2 + P_2 = c_2 \tag{2}$$

$$\tfrac{1}{2} u_1^2 + h_1 = \tfrac{1}{2} u_2^2 + h_2 = c_3 - \Delta Q_{\text{rad}} \tag{3}$$

where ρ is the mass density, u the flux velocity, P the pressure, h the total entalpy, and the subscripts $i = 1,2$ refers to the upstream and downstream variables respectively. The term ΔQ_{rad} in the energy equation accounts for radiative energy losses that in our model are limited to spontanous emission and radiative recombination.

The enthalpy h is made up of a traslational and an internal contribution

$$h_T = c_P T \tag{4}$$

$$h_{\text{int}} = \sum_s \left(h_{fs} + \sum_i \varepsilon_{si} \chi_{si} \right) x_s \tag{5}$$

where c_p is the total specific heat at constant pressure per unit mass, T the gas temperature, h_{fs} the formation enthalpy of the $s-$th specie, ε_{si} the energy of the $i-$th internal level of the $s-$th specie with χ_{si} the corresponding molar fraction and x_i the mass fraction of the specie. The system (1–3) is closed using the perfect gas equation of state.

Collisional-radiative model

The composition and level population of the (H,H^+,e^-) plasma at each spatial point have been determined with a collisional-radiative model. The model solves a system of rate equations, one for each internal level, taking into account the rate coefficients of the most relevant collisional and radiative processes. Only collisional processes promoted by free electrons have been considered, neglecting heavy-heavy collisions. The included processes are: excitation/de-excitation by electron impact, ionization and three-body recombination, spontaneous emission and absorption and radiative recombination. The resulting system of equations is

$$\begin{cases} \dfrac{\mathrm{d}N_{n'}}{\mathrm{d}t} = -N_{n'} \displaystyle\sum_{j<n'} A^*_{n'j} + \sum_{j>n'} N_j A^*_{jn'} - N_{n'} N_{\text{e}} \sum_{\substack{j=1 \\ j\neq n'}} k_{n'j} + N_{\text{e}} \sum_{\substack{j=1 \\ j\neq n'}} N_j k_{jn'} \\ \qquad\qquad + N_e^2 N_{\text{H}^+} k_{rn'} - N_{n'} N_{\text{e}} k_{n'i} + N_{\text{e}} N_{\text{H}} \beta_{n'} \qquad n' = 1,\ldots,25 \\ \dfrac{\mathrm{d}N_+}{\mathrm{d}t} = \dfrac{\mathrm{d}N_e}{\mathrm{d}t} = -\displaystyle\sum_{n'} \frac{\mathrm{d}N_{n'}}{\mathrm{d}t} \end{cases} \tag{6}$$

where n' is the principal quantum numbers of the atomic states, $k_{n'n}, k_{nn'}$ the excitation and de-excitation rate coefficients in cm^3s^{-1}, $k_{n'i}, k_{rn'}$ the ionization and three body recombination rate coefficients in cm^3s^{-1} and cm^6s^{-1}, $A_{nn'}$ (s^{-1}) the Einstein coefficient for spontanous emission and $\beta_{n'}$ the rate coefficient for radiative recombination in cm^3s^{-1}. Electron impact rate coefficients have been calculated from the relevant cross sections and the electron energy distribution function (EEDF), the latter obtained by the solution of the electron Boltzman equation:

$$\frac{\mathrm{d}f_{\text{e}}(\varepsilon,t)}{\mathrm{d}t} = -\frac{\mathrm{d}J_E}{\mathrm{d}\varepsilon} - \frac{\mathrm{d}J_{\text{el}}}{\mathrm{d}\varepsilon} - \frac{\mathrm{d}J_{\text{e-e}}}{\mathrm{d}\varepsilon} + S_{\text{in}} + S_{\text{sup}} \tag{7}$$

where $\frac{\mathrm{d}f_{\text{e}}(\varepsilon,t)}{\mathrm{d}t}$ is the rate of change of the EEDF at a given energy ε, and J_E, J_{el}, $J_{\text{e-e}}$ are flux terms in the electron energy space due to electric field, elastic collisions with atom and ions and electron-electron elastic collisions respectively. S_{in} and S_{sup} are the source terms due to inelastic and superelastic collisions. The inelastic processes correspond to electron impact excitation and ionization, while superelastic ones to de-excitation and recombination.

Radiative transfer equation

Radiative transfer has been described using the following non-scattering axisymmetric 1D radiative transfer equation (RTE) in slab geometry

$$\mu \frac{dI_\nu(x,\mu)}{dx} = j^e_\nu(x) + \kappa'_\nu(x) I_\nu(x,\mu) \tag{8}$$

where $I_\nu(x,\mu)$ is the radiation intensity in erg cm^{-2}s^{-1}sr^{-1}Hz^{-1} propagating along a ray with director cosine μ with respect to the $x-$axis. The term $j^e_\nu(x)$ is the spectral emissivity in erg cm^{-3}s^{-1}sr^{-1}Hz^{-1}, while $\kappa'_\nu(x)$ is the absorption coefficient corrected for stimulated emission. These coefficients are calculated from the local level densities, taking into account the bound-bound, bound-free and free-free radiative processes. For bound-bound processes the most important line broadening effects have been taken into account [6, 7, 8, 9], even if the modelling of the first Balmer (and probably Lyman) lines should be improved [2] to obtained a better agreement with experiment.

Once the RTE has been solved, other important quantities can be calculated [3]

$$J_\nu(x) = \frac{1}{2}\int_{-1}^{1} I_\nu(x,\mu)d\mu \tag{9}$$

$$q_\nu(x) = 2\pi \int_{-1}^{1} I_\nu(x,\mu)\mu d\mu \tag{10}$$

$$\frac{dq_\nu}{dx} = 4\pi \left(j^e_\nu(x) - \kappa'_\nu J_\nu(x)\right) \tag{11}$$

where J_ν, $q_\nu(x)$ and $dq_\nu(x)/dx$ are spectral average intensity, radiative flux and radiative flux divergence respectively.

RESULTS

In this section, we present results obtained by imposing the following initial conditions in the preshock region: $P_1 = 10^{-2}$ atm, $T_{\rm gas} = 1000$ K, $\chi_{\rm H} = 1$, $\chi_{\rm H^+} = \chi_{e^-} = 10^{-10}$, $M_1 = 20$ mach. The $x = 0$ coordinate is set at the shock front, while preshock and postshock regions are at $x < 0$ and $x > 0$respectively.

In figure 1 the spatial distributions of H,H$^+$ and e$^-$ and $T_{\rm gas}$, T_e and $T_{\rm H}$ are reported. The internal H atom temperature has been calculated as the temperature of a Boltzmann distribution fitting the actual populations of the ground and first excited levels. Two distinct phases can be identified in the post shock: a ionization and a recombination one. These two regimes are linked to the gas temperature space distribution, characterized by a sudden increase just after the shock front, while after a certain distance, radiative losses dominate causing the progressive cooling of the gas. In the ionization region $T_{\rm H}$ and $T_{\rm e}$ is lower than $T_{\rm gas}$ but both reach Tgas at the point corresponding to the maximum of H^+ and e^- density. After this point $T_{\rm e}$ remains approximately equal to $T_{\rm gas}$ since e^-–H^+ collisions are quite effective in equilibrating the two temperatures. On the other hand T_H decreases to a lower value due to the effect of radiative losses. It should be remarked that because we neglect atom-atom ionizations processes and direct photoionization of neutral atoms, the electron density increase rate is underestimated, and the position of the ionization maximum should be nearest to the shock front than predicted by our model.

In figure 2 (a) the internal atom distributions are reported at different space points. In the ionization region, corresponding to curves 1–3, non-equilibrium distribution, characterized by underpopulation of higher excited states are shown. Curve 4, corresponding to the electron density peak of about $7\,10^{17}$ cm^{-3} shows that at this point equilibrium has been reached. After that distributions start to cool down, deviating from the Boltzmann distribution due to a slight overpopulation of higher levels characteristic of the recombination regime.

An analogous trend is observed in the EEDF curves. In the ionization phase an underpopulation of the high energy tail of the distributions can be observed. At the maximum electron density point, currespnding to curves 4 and 5, the EEFD is essentially Maxwell, while in the recombination regime (curves 6–9), superelastic collisions (electron impact de-excitation of atoms) lead to a peak of the distribution at 10.2 eV corresponding the supereleastic collision between the $n = 2$ to $n = 1$ states of atomic hydrogen.

In figure 3 the kinetic energy flux $F_K = \frac{1}{2}c_1 u^2$, the entalphy flux $F_h = (h_T + h_{\rm int})c_1$ and the radiative flux defined in eq. (10) are reported as a function of the spatial coordinate. The kinetic energy flux shows a sudden decrease across the shock front due to the jump in the flow velocity, while the enthalpy flux increases with the gas temperature $T_{\rm gas}$. On the other hand the radiative flux abruptly changes sign near the point of maximum ionization and excitation of internal

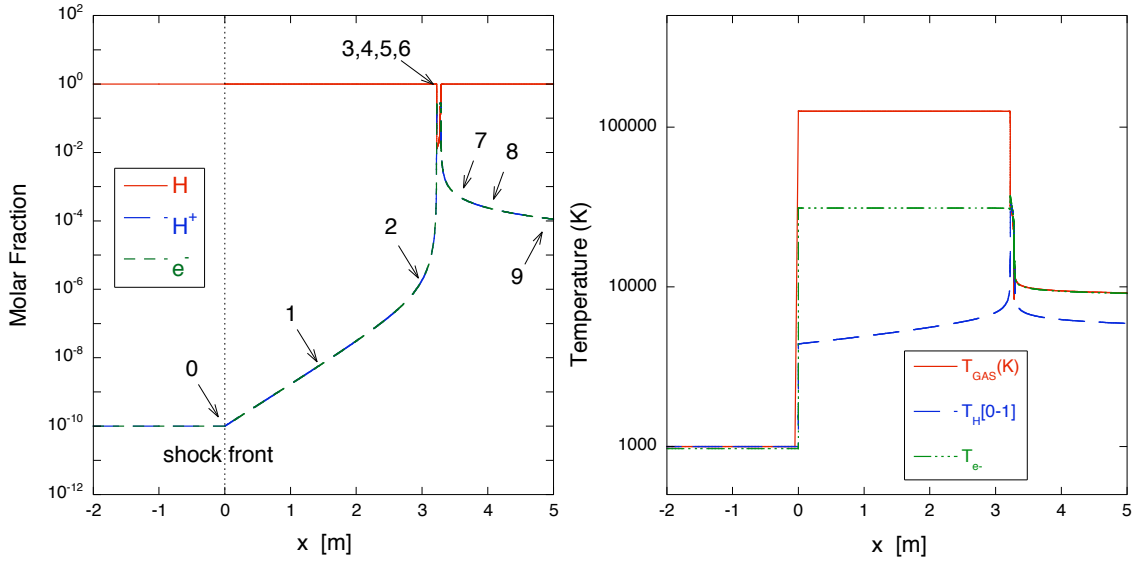

FIGURE 1. Spatial distribution of a) molar fractions of H,H^+, e^- and b) $T_{\rm gas}$, T_e and $T_{\rm H}$ in the shock wave propagating through partially ionized hydrogen gas with upstream conditions characterized by $P_1 = 10^{-2}$ atm, $T_{\rm gas} = 1000$ K, $\chi_{\rm H} = 1$, $\chi_{\rm H^+} = \chi_{e^-} = 10^{-10}$, $M_1 = 20$. The numers refers to the following coordinate values (m): $x_0 = 0$, $x_1 = 1.5$, $x_2 = 3$, $x_3 = 3.2189$, $x_4 = 3.27959$, $x_5 = 3.28689$, $x_6 = 3.29642$, $x_7 = 3.50227$, $x_8 = 4.00199$, $x_9 = 5$.

states. It is worth noting that a negative sign of the radiative flux means a net flux of radiation propagating from right to left, while a positive sign implies that radiation is propagating from left to right. The rapid variation of the radiative flux is a consequence of the large absorption cross section ($10^1 \div 10^3$ cm^{-1}) near the point of maximum ionization.

In figure 4 the local source function $S_\nu = j^e_\nu / \kappa'_\nu$ computed using the actual densities and temperatures of the CR model is reported at the x-positions marked as 5 and 6 in figure 1. By the Kirchhoff-Planck relation, this quantity equals the blackbody intensity $B_\nu(T)$ at thermodynamic equilibrium, and remains very close to $B_\nu(T)$ in LTE [3]. In figure 4 the function $B_\nu(T)$ calculated at the local $T_{\rm gas}$ is also reported.

Figure 4 shows that the S_ν distribution is nearly equilibrium at point 5, characterized by a Boltzmann level distribution and by a Maxwell EEDF, see figure 2. At point 6 the recombination phase has just started with the consequence that the spectral region of Lyman lines and ground state photoionization is below the equilibrium distribution. This is due to both a reduction of emissivity, as a consequence of the decreased population of excited states number density, and an increase of the absorption coefficient of radiative transitions starting from the ground state.

CONCLUSIONS

A model for the simulation of the spectra emitted by an hydrogen plasma in shock wave conditions has been described. The model solves the steady state shock wave continuity equations taking into account radiative losses due to spontaneous emission and radiative recombination. Non-equilibrium has been accounted using a state-to-state approach (CRM) for excited level populations and the free-electron Boltzmann equation for electron energy distribution function. The radiative flux and has been obtained through solution of the one-dimensional radiative transfer equation.

In the post shock flow a ionization a a recombination regions are observed, each one characterized by non-equilibrium internal level and EEDF distributions leading to corresponding non-equilibrium spectral distribution. A small intermediate region where distributions are nearly equilibrium, located between the ionization and recombination regions has been found, corresponding to the maximum of the ionization degree.

Future developements include the coupling of the radiative transfer equation with the Collisional-Radiative model to calculate rates for radiative processes self-consistently with the radiation field. The kinetic model will be improved

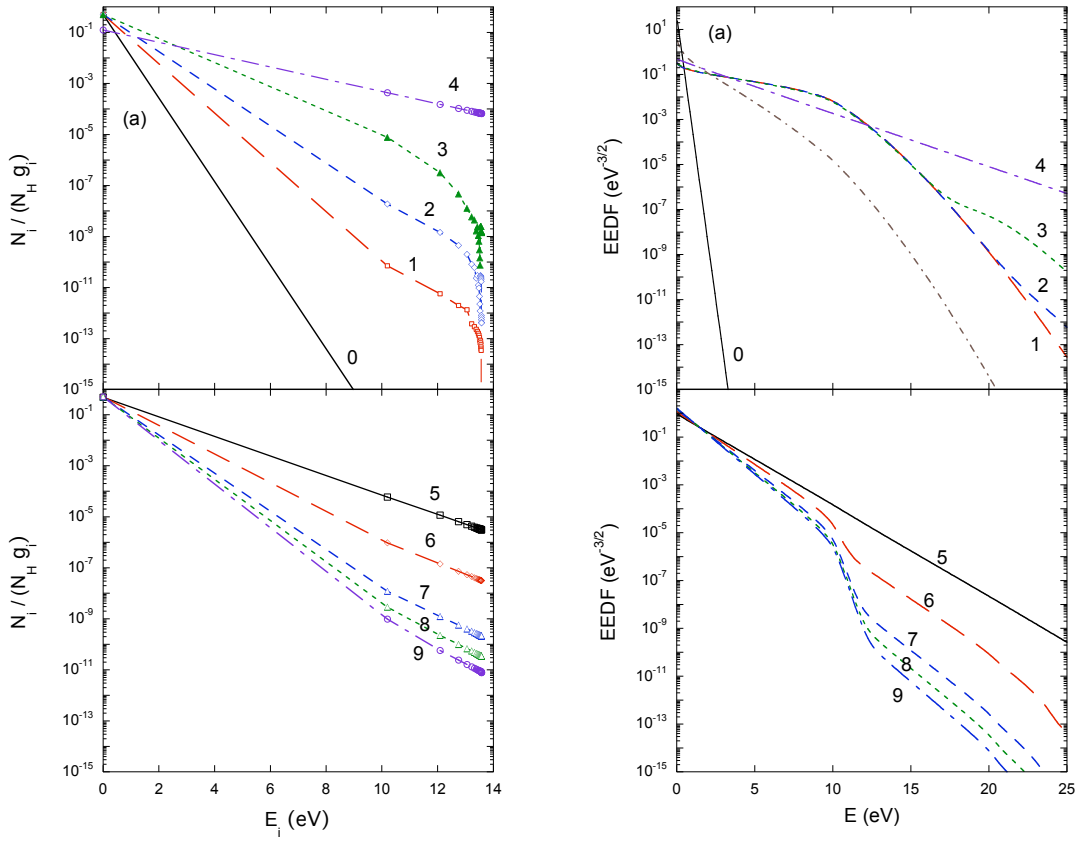

FIGURE 2. (a) H level populations distribution as a function of the level energy and (b) electron energy distributions a a function of electron kinetic energy at various spatial positions. Numbers refer to the space positions reported in figure 1.

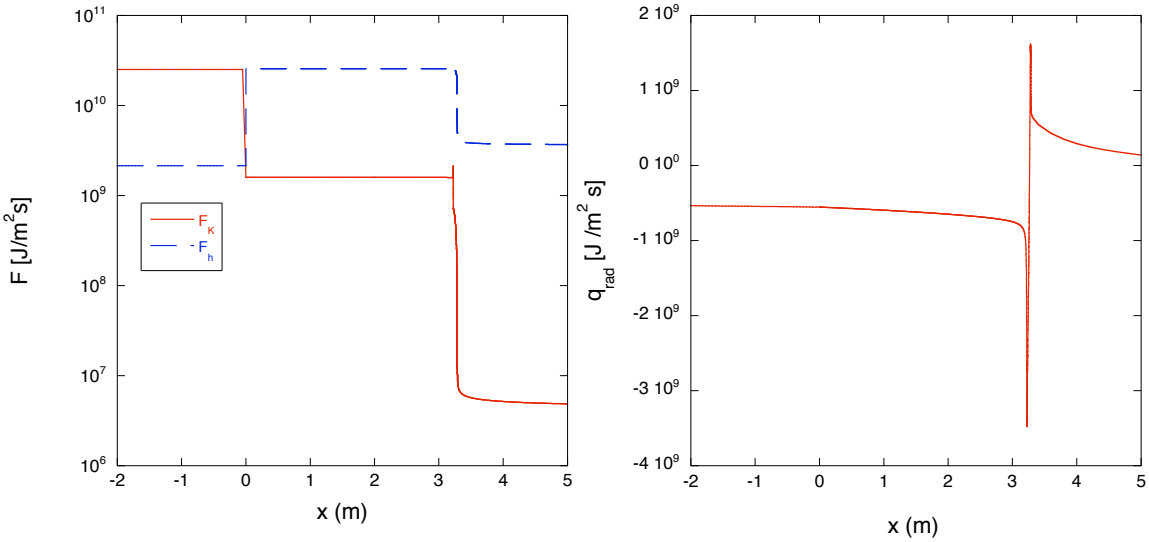

FIGURE 3. Kinetic and entalpy energy fluxes (a) and radiative energy flux (b) as a function of position.

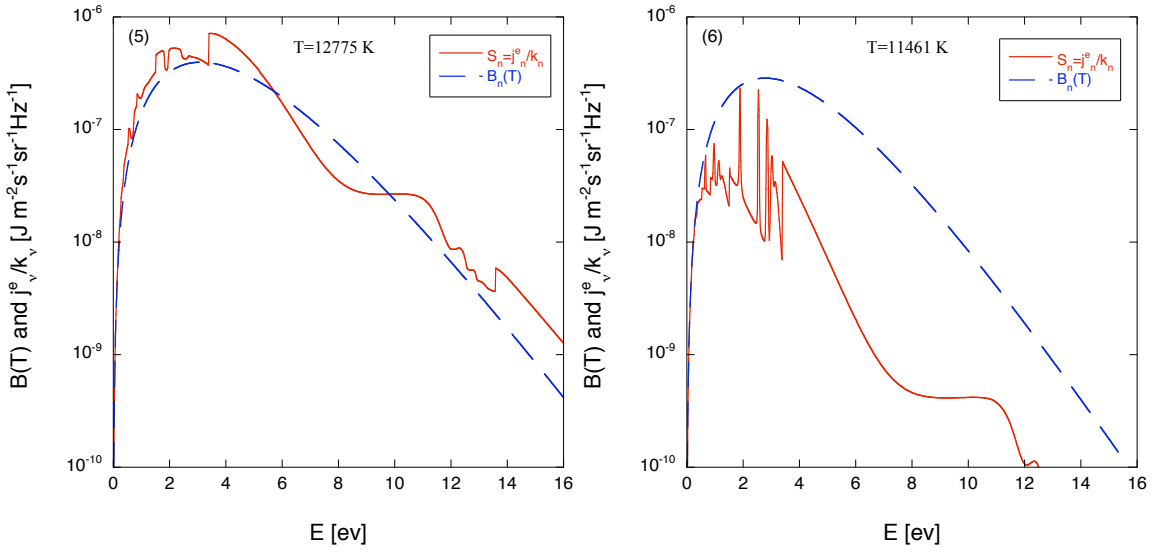

FIGURE 4. Local spectral source function $S_\nu = j^e_\nu / 1\kappa'_\nu$ at two difference spatial positions after the shock front, compared to the corresponding equilibrium distribution at the local value of $T_{\rm gas}$. Numbers refer to the space positions reported in figure 1.

by including atom-atom impact ionization and photo-ionization for a more realistic description of the ionization phase. Finally, to extend the validity region of the model towards lower gas temperatures, a model for H_2 level kinetics should be implemented.

ACKNOWLEDGEMENTS

The research leading to these results has received funding from the European Community's Seventh Framework Programme (FP7/2007-2013) under grant agreement n. 242311.

REFERENCES

1. G. Colonna, L. D. Pietanza, and M. Capitelli, *Spectrochimica Acta Part B* **56**, 587–598 (2001).
2. G. D'Ammando, L. D. Pietanza, G. Colonna, S. Longo, and M. Capitelli, *Spectrochimica Acta Part B: Atomic Spectroscopy* **65**, 120–129 (2010).
3. D. Mihalas, and B. Weibel Mihalas, *Foundations of Radiation Hydrodynamics*, Oxford University Press, 1984.
4. Y. A. Fadeyev, and D. Gillet, *Astron. Astropys.* **368**, 901–911 (2001).
5. Y. A. Fadeyev, and D. Gillet, *Astron. Astropys.* **354**, 349–364 (2000).
6. H. R. Griem, *ApJ* **148**, 547–588 (1967).
7. H. R. Griem, *Principles of Plasma Spectroscopy*, Cambridge Monographs on Plasma Physics, Cambridge university press, 1997.
8. I. Sobel'man, L. A. Vainsthtein, and E. A. Yukov, *Excitation of atoms and brodening of spectral lines*, Springer-Verlag, 1995.
9. S. Surzhikov, M. Capitelli, G. Colonna, and C. Gorse, *Journal of Thermophysics and Heat Transfer* **22**, 62–70 (2008).